Nonlinear static procedures for state-dependent seismic fragility analysis of reinforced concrete buildings

Livio Pedone[1], Roberto Gentile[2,3], Carmine Galasso[3,4], Stefano Pampanin[1]

[1]Department of Structural and Geotechnical Engineering,
Sapienza University of Rome,
Via Eudossiana 18, 00184, Rome, Italy

[2]Institute for Risk and Disaster Reduction,
University College London,
Gower Street, WC1E 6BT, London, United Kingdom

[3]Department of Civil, Environmental and Geomatic Engineering,
University College London,
Gower Street, WC1E 6BT, London, United Kingdom

[4] Scuola Universitaria Superiore IUSS Pavia,
Piazza della Vittoria 15, 27100, Pavia, Italy

Abstract
This paper introduces a simplified methodology to develop state-dependent fragility relationships, based on nonlinear static analyses combined with the Cloud Capacity Spectrum Method. Capacity reduction factors for structural members are applied to simulate the attainment of a specific damage state under a mainshock. A cloud-based procedure is adopted to compute fragility analyses. The procedure is illustrated for a case-study building designed for gravity loads only. Results highlight the importance of considering the effect of cumulative damage in the fragility analysis of buildings. The proposed methodology may be used for seismic-risk assessment studies accounting for ground-motion sequences.

1 Introduction and motivation

In earthquake-prone countries, ground-motion sequences clustered in space and time are typically observed. Recent earthquakes, such as the 2010-2011 Canterbury earthquake sequence [1] and the 2016–2017 Central Italy earthquake sequence, have further highlighted the potentially catastrophic consequences of sequential earthquake-induced ground shaking. After a mainshock (MS), buildings may be characterised by substantial structural damage, and, as a result, loss of their lateral-force resisting capacity may occur. Therefore, assessing the residual capacity of earthquake-damaged buildings to sustain subsequent aftershocks (AS) is critical to assess seismic risk in post-earthquake scenarios to support decision-making related to both re-occupancy and repair vs demolition.

In the past decades, significant research efforts have been devoted to better understand the seismic performance and fragility of mainshock-damaged buildings. In the Federal Emergency Management Agency (FEMA) 306 report [2], a practical pushover-based approach for evaluating the effects of structural damage on concrete and masonry-wall buildings is proposed. Specifically, damaged building behaviour is simulated by adopting a modification of the nonlinear capacity curve (i.e., force-deformation or moment–rotation relationships) of damaged elements based on stiffness, strength, and ductility reduction coefficients, namely λ_k, λ_Q, and λ_D. A conceptually-similar approach is also proposed in the Japan Building Disaster Prevention Association (JBDPA) Guideline [3], where a single capacity reduction factor for structural members is adopted, defined as the ratio between residual energy dissipation capacity and original energy dissipation capacity. Moving to fragility analysis, the concept of state-dependent fragility relationships (i.e., fragility relationships depending on the attained damage state after a MS) must be adopted to consider the effects of ground-motion sequences explicitly. According to state-of-the-art procedures in the literature, the most reliable approach for seismic fragility analysis

involves the use of nonlinear dynamic analyses of a Multi-Degree-of-Freedom (MDoF) numerical model of the structure of interest (e.g., [4]-[8]). However, deriving state-dependent fragility relationships through nonlinear dynamic procedures, such as back-to-back incremental dynamic analyses (IDA), typically requires significant computational effort. For many practical applications (e.g., those involving a large building portfolio), simplified approaches are often required/preferred [9]. For example, Orlacchio et al. [10] recently proposed a pushover-based methodology to estimate state-dependent fragility relationships. A semi-empirical predictive model is adopted to define the mainshock-damaged force-displacement curve of an equivalent Single-Degree-of-Freedom (SDoF) system. Then, state-dependent fragilities are estimated via IDA for those SDOF systems. Moreover, following the FEMA 306 approach, Polese et al. [11] proposed a methodology to develop damage-dependent collapse fragility curves based on a spectral approach, i.e., by applying the incremental N2 method (IN2, [12]) considering the structure in its as-built and damaged configuration. It is worth noting that default fragility dispersion values are adopted, and only the median values of the fragility curves are explicitly derived. A simplified and practical procedure to develop state-dependent fragility relationships considering record-to-record variability is still missing in the literature.

Therefore, this paper introduces a novel simplified methodology to develop state-dependent fragility relationships. Firstly, a refined lumped plasticity modelling approach is adopted, and nonlinear static analyses are performed to assess the force-displacement capacity curves of the structure in its damaged and undamaged configuration. Specifically, the achievement of a specific damage state after a mainshock is simulated by using capacity reduction factors for damaged structural members, according to the FEMA 306 approach. Then, the seismic performance of the as-built and damaged configurations is evaluated by applying an extension of the Capacity Spectrum Method (CSM, [13]), i.e. the Cloud-CSM [14]. This methodology uses "real" (i.e., recorded) ground motions and allows explicitly accounting for record-to-record variability in fragility analysis. Finally, state-dependent fragility relationships are derived for each damage state via cloud analysis. A detailed description of the procedure is reported in section 2. In section 3, the procedure is illustrated for a case-study building designed for gravity loads only, while conclusions are given in section 4.

2 Methodology

The proposed framework for developing state-dependent fragility relationships is illustrated in Fig. 1, referring to an RC frame structure (however, the framework may be applied to other structure typologies as well). Each step is discussed in detail below.

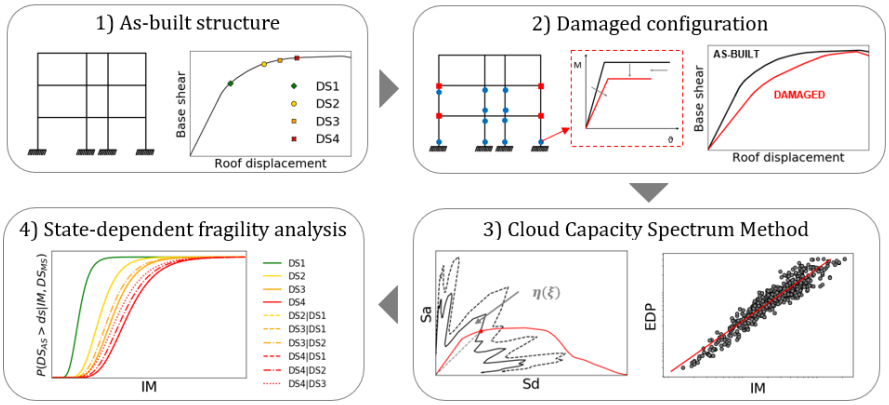

Fig. 1 Proposed flowchart for developing state-dependent fragility relationships

The main steps of the procedure are reported and discussed below:

1) Building model and pushover analysis for the as-built structure (step1):

Geometric details and material properties of the case-study structure are defined. The seismic behaviour of the as-built configuration is assessed by adopting a lumped plasticity modelling approach and performing nonlinear static (pushover) analysis. Moreover, different structure-specific damage states

(DSs) are defined based on the pushover analysis results. More details about the modelling approach adopted in this work as well as the considered DSs are reported in section 3.3 and section 3.4, respectively. It is worth noting that the proposed framework is independent of the DSs definition, and different criteria can be adopted.

2) Seismic behaviour of the damaged structure (step 2):

The seismic behaviour of the structure in its post-earthquake (i.e., damaged) condition is evaluated according to the FEMA 306 approach and the framework proposed in [11]. For each considered damage state, the local ductility demand for the elements that have exceeded the yielding deformation is evaluated, and suitable reduction factors for their plastic hinges' response are selected to simulate the seismic behaviour of the damaged structure. The modification factors proposed by Di Ludovico et al. [15] are adopted. These plastic hinges modification factors are provided as a function of the rotational ductility demand and were derived considering a database of cyclic test results on typical non-conforming RC members of buildings in Mediterranean regions. Therefore, different nonlinear models are obtained for each DS. The nonlinear capacity curve of the "damaged" elements is modified in terms of stiffness, strength, and plastic rotation capacity (Fig. 1, step 2). Additional nonlinear static analyses are thus performed to assess the seismic behaviour of the structure in its damaged conditions.

3) Seismic response analysis of the as-built and damaged structure via Cloud-CSM (step 3)

Seismic response analyses of the as-built and damaged structure are performed by using numerical pushover capacity curves coupled with the Cloud-CSM, following the procedure proposed in [14]. As mentioned above, this method is an extended version of the traditional CSM that allows explicitly considering record-to-record variability, using as-recorded spectra instead of a code-base spectrum. More details about the ground motion selection are reported in section 3.2. The equivalent viscous damping (ξ) and the spectral reduction factor (η) are calculated according to [16]. Performance points of the as-built and damaged structure are determined considering each selected ground motion. It is worth noting that multiple performance points may be obtained when using real ground-motion spectra. In this study, the performance point corresponding to the smallest displacement is considered in the case of multiple solutions. As shown in [14], this selection approach shows a satisfactory accuracy without increasing the calculation effort. An engineer demand parameter (EDP) vs intensity measure (IM) cloud is thus obtained for each configuration.

4) State-dependent fragility analysis (step 4)

The cloud-based procedure proposed by Jalayer et al. [17] is finally adopted to compute fragility analyses. Specifically, the cloud data are divided into "collapse" (C) and "no-collapse" (NoC) cases. Collapse cases correspond to no-intersection between the pushover capacity curve of the structure and the earthquake demand (i.e., the considered ground-motion spectra) in the Acceleration Displacement Response Spectra (ADRS) domain. Using the total probability theorem, the state-dependent fragility relationships can be expressed as:

$$P(EDP \geq edp_{DS}|DS_{MS}, IM_{AS}) = P(EDP \geq edp_{DS}|DS_{MS}, IM_{AS}, NoC)\big(1 - P(C|DS_{MS}, IM_{AS})\big) + P(C|DS_{MS}, IM_{AS}), \quad (1)$$

where $P(EDP \geq edp_{DS}|DS_{MS}, IM_{AS}, NoC)$ is the probability of exceeding a specific EDP threshold given a DS in the MS and given that collapse does not occur; $P(C|DS_{MS}, IM_{AS})$ is the probability of collapse, given a DS in the MS. It is worth noting that Eq. (1) assumes that $P(EDP \geq edp_{DS}|DS_{MS}, IM_{AS}, C) = 1$. The linear least square method is applied on the NoC cloud data to derive the power-law probabilistic seismic demand model $EDP = aIM^b$ for the as-built and the damaged structure. Therefore, $P(EDP \geq edp_{DS}|DS_{MS}, IM_{AS}, NoC)$ is represented by a lognormal cumulative distribution function (CDF). A logistic regression model (suitable to binary variables, as collapse-no collapse) is fitted to calculate $P(C|DS_{MS}, IM_{AS})$, considering each initial DS. Finally, the result is converted into a lognormal CDF, defined by a median and a logarithmic standard deviation, according to [18].

The following section demonstrates the proposed framework for an RC case-study building typical of the Italian regions.

3 Illustrative application

3.1 Case-study building

The considered case-study building is a 3-story RC structure with global dimensions and plan geometry shown in Fig. 2. The structural skeleton consists of moment-resistant three-bay frames in one direction and moment-resistant two-bay frames in the orthogonal direction. This structure represents an archetype pre-1970s building in the Italian region, i.e. designed for gravity load only. Therefore, neither lateral-load design and capacity design principles are provided, and the structure presents the typical structural weaknesses of buildings designed in that period (e.g., strong beam/weak column, inadequate transverse reinforcement for shear and confinement, inadequate anchorage details, lower quality of materials). In this study, the central longitudinal frame is analysed. Geometrical details of RC members are reported in Fig. 2 (right).

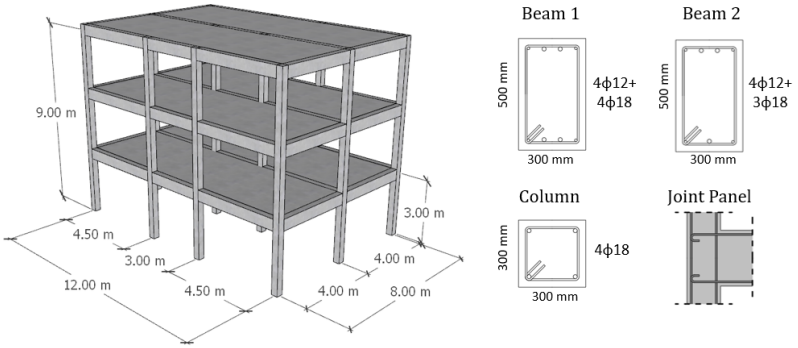

Fig. 2 Global view of the case-study building (left) and geometrical details of RC members (right)

The beam-column joint presents no stirrups and plain round beam bars with end-hooks. Columns and beams present a transverse reinforcement of $\phi 6/15$ and $\phi 8/15$, respectively. The mean concrete cylindrical strength is equal to 14.41 MPa, and the mean steel yield stress is equal to 340.51 MPa.

3.2 Ground-motion selection

A set of 621 recorded ground motions (Fig. 3) is selected to perform fragility analysis using the Cloud-CSM. The ground motion records are selected from three different databases ([7]; [8]): (1) the 2012 KKiKSK ground-motion database [19]; (2) the database developed by Goda and Taylor [20]; and (3) the 100 records with the highest peak ground acceleration (PGA) in the SIMBAD Database [21]. Only the MS from the previous two databases are considered. Information about magnitude and source-to-distance values, soil types, and PGA values for the considered records are reported in [7]. It is worth noting that the cloud-based response analysis approach does not require a hazard-consistent suite of ground-motion records. Moreover, cloud analysis does not require ground-motion scaling, overcoming all the related issues. Unlike [7] and [8], the proposed methodology does not require ground-motion sequences as the Cloud-CSM is only performed for the AS (Fig. 1, step 3).

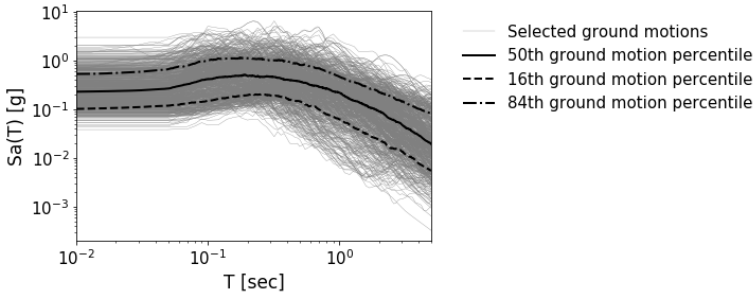

Fig. 3 Ground-motion response spectra

3.3 Modelling approach

A refined two-dimensional (2D) lumped plasticity model is implemented in the finite-element software Ruaumoko [22] to develop nonlinear static pushover analyses. Floor diaphragms are assumed rigid in their plane, while fixed base joints are introduced (i.e., the soil-structure interaction contribution is neglected). The RC members are modelled by mono-dimensional elastic elements with plastic hinges at the connection interfaces (Giberson elements). Proper bi-linear moment-curvature relationships characterise beam plastic hinges. The plastic hinge length is calculated according to [16]. An axial load-moment interaction diagram characterises column plastic hinges. The shear failure mechanism is also evaluated. The Takeda hysteresis is adopted for beams and columns. Panel zones are modelled using rigid arms with additional nonlinear rotational springs to consider possible failure mechanisms [23]. The springs are characterised by equivalent column moment versus drift relationships [24]. Moreover, an axial load-moment interaction diagram is implemented to consider the influence of the axial load in the beam-column joint capacity. The modified Sina model [25] is adopted for beam-column joints, allowing one to consider a pinching behaviour. Finally, a linear strength degradation for RC members is defined. Specifically, the moment capacity is set equal to zero when twice of near-collapse deformation capacity of the member is achieved.

3.4 Result and Discussion

3.4.1 Nonlinear static analyses

The nonlinear static analysis result for the as-built structure is reported in Fig. 4 (left) in terms of the force-displacement capacity curve. As expected, the as-built structure shows a low global ductility behaviour. Due to the lack of capacity-design principles, a mixed-sway mechanism is observed, characterised by external beam-columns joint failures coupled with columns failures. Moreover, Fig. 4 (left) shows the DS thresholds adopted for the fragility analysis. In this study, four different DSs are considered, namely: DS1 (slight damage), DS2 (moderate damage), DS3 (extensive damage), and DS4 (complete damage). Specifically, DS1 corresponds to the yield displacement of the idealised pushover curve; DS2 refers to the first structural element reaching 50% of its life-safety plastic deformation capacity; DS3 and DS4 correspond to the first attainment of life-safety and collapse prevention limit state for any structural element, respectively. The corresponding DS thresholds in terms of maximum inter-storey drift ratio are thus derived from the numerical analysis results. Then, for each considered damage state, suitable reduction factors for the plastic hinges' response of damaged members are selected as a function of their rotational ductility demand. Therefore, four additional nonlinear models are obtained (i.e., one for each DS). The results of nonlinear static analyses of the structure in its damaged conditions are shown in Fig. 4 (right).

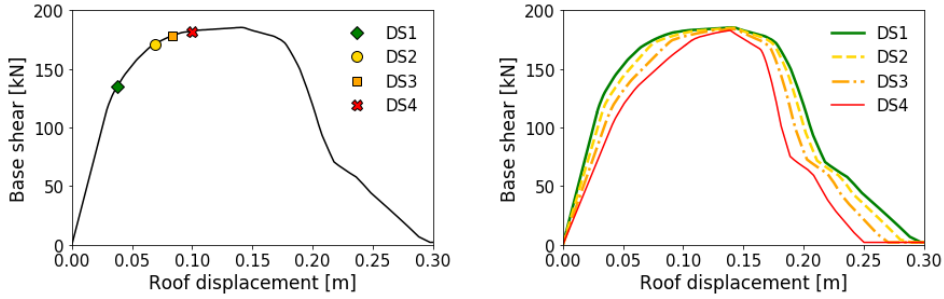

Fig. 4 Capacity curves of the as-built (left) and damaged (right) structure configurations

3.4.2 Seismic response and fragility analyses

Seismic response analysis for the undamaged and damaged structure configurations are computed following the pushover-based Cloud-CSM. Capacity curves are converted into acceleration–displacement curves in the ADRS domain. Effective height, effective mass, and equivalent viscous damping formulations provided by Priestley et al. [16] are adopted. No bilinearisation of the capacity curve is considered. The Cloud-CSM is applied for each DS, using the 621 ground-motion response spectra previously

selected. Results in terms of performance points are illustrated in Fig. 5 (left). The corresponding maximum inter-storey drift ratio (MIDR) is calculated using the displacement profile obtained from the pushover analyses. Therefore, an EDP (i.e., MIDR) vs IM cloud is derived for the as-built structure and each DSs. In this study, the adopted IM is the geometric mean (avgSA) of the pseudo-spectral acceleration in a specific range of periods depending on the first-mode periods of the structure. As an example, Fig. 5 (right) shows the results of the seismic response analysis and the obtained power-law probabilistic seismic demand model (PSDM) for the DS3 configuration. A comparison between the PSDM of the undamaged and DS3 configurations is also reported. As expected, considering the same IM, higher drift values are obtained for the DS3 configuration when compared to the undamaged configuration.

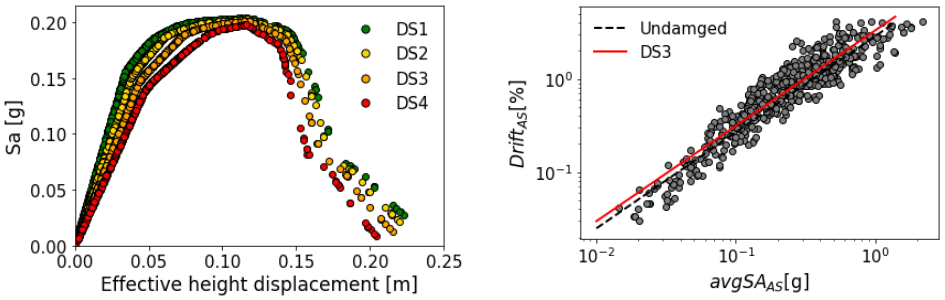

Fig. 5 Performance points of the structure in its damaged configurations (left) and seismic response analysis results for the DS3 configuration (right).

Finally, state-dependent fragility relationships are derived. Fig. 6 (left) shows the fragility curves derived for the undamaged case-study structure. State-dependent fragilities curves are shown in Fig. 6 (right). Moreover, median and standard deviation values of state-dependent fragility curves of state-dependent fragility curves are listed in Table 1.

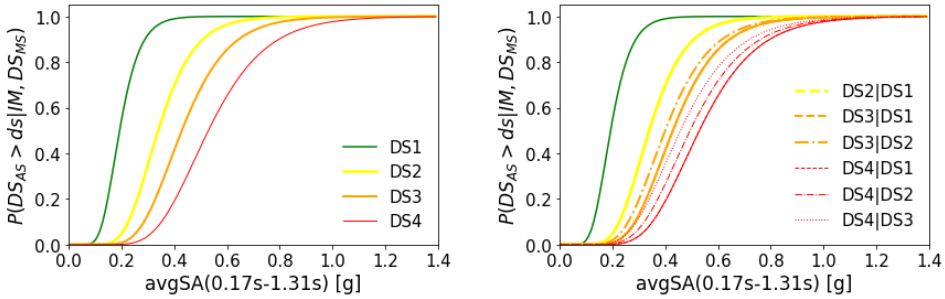

Fig. 6 Undamaged state fragility curves (left) and state-dependent fragility curves (right).

Table 1 Median and standard deviation values of state-dependent fragility curves

		Initial DS due to the mainshock							
		As-built		DS1		DS2		DS3	
		$\mu_{DS}[g]$	β	$\mu_{DS}[g]$	β	$\mu_{DS}[g]$	β	$\mu_{DS}[g]$	β
Conditional DS	DS1	0.193	0.315	-	-	-	-	-	-
	DS2	0.339	0.317	0.339	0.317	-	-	-	-
	DS3	0.429	0.318	0.429	0.318	0.400	0.336	-	-
	DS4	0.529	0.319	0.529	0.319	0.494	0.337	0.458	0.354

As can be noted, a low level of damage (i.e., DS1) does not significantly modify the structural behaviour of the structure. Therefore, no significant shift of the aftershock fragilities is observed for initial DS1 due to a mainshock. On the other hand, the presence of more severe initial damage (i.e., DS2, DS3) increases the fragility of the structure. Specifically, a reduction equal to 7% is observed for the DS3|DS2 and DS4|DS2 fragility median, while the DS4|DS3 fragility median is reduced by 14%. No fragility

curve crossings between various DSs are observed. It is worth remembering that the reference structure is a pre-1970s building, showing a low seismic performance. Therefore, it could be observed that damage accumulation could be considered less relevant since the building may not respect the code seismic-performance standards even in its undamaged configuration. However, the increased fragility due to initial earthquake damage may significantly affect retrofit/repair vs demolition decision-making in a post-earthquake scenario.

4 Conclusions

In this paper, a simplified methodology to develop state-dependent fragility relationships for structures subjected to mainshock-aftershock ground motion sequences was presented. The procedure is based on nonlinear static analyses combined with the Cloud Capacity Spectrum Method. The seismic performance of the structure in its post-earthquake (i.e., damaged) condition is evaluated by using suitable capacity reduction factors for damaged structural members, according to the state-of-the-art of procedures available in the literature. Seismic response analyses are performed for each DS according to the Cloud-CSM. This methodology is based on natural, as-recorded ground motions and allows explicitly accounting for record-to-record variability in fragility analysis. The proposed framework was illustrated for a case-study RC frame designed for gravity loads only. The results from such an application confirm the feasibility of the proposed methodology. The effects of damage accumulation were captured without statistical inconsistencies (e.g., no fragility curve crossings between various DSs were observed). An increasing reduction of the fragility median was obtained as initial damage due to a mainshock increased.

The proposed methodology may be used for seismic-risk assessment studies accounting for ground-motion sequences. It may support the decision-making process of both re-occupancy and repair vs demolition in post-earthquake scenarios. It is worth mentioning that future, more-refined numerical investigations (e.g., nonlinear time history analyses) are needed to better validate the proposed framework. Moreover, a broader class of frame structures can be used to improve the study, including newly-designed RC frame structures and infilled frame structures.

Acknowledgements ??

The authors acknowledge the financial support of the Italian Ministry of Education, University and Research (MIUR) for funding the Doctoral Scholarships of Livio Pedone. Roberto Gentile received funding from the European Union's Horizon 2020 research and innovation programme: Marie Skłodowska-Curie Research Grants Scheme MSCA-IF-2018: 843794.

References

[1] Kam, Weng Y., Stefano Pampanin, and Ken Elwood. 2011. "Seismic Performance of Reinforced Concrete Buildings in the 22 February Christchurch (Lyttelton) Earthquake." *Bulletin of the New Zealand Society for Earthquake Engineering* 44 (4): 239–78. https://doi.org/10.5459/bnzsee.44.4.239-278.

[2] Federal Emergency Management Agency. 1998. *Evaluation of Earthquake Damaged Concrete and Masonry Wall Buildings – Basic procedures manual*. FEMA 306, Washington DC.

[3] Nakano Yoshiaki, Masaki Maeda, Hiroshi Kuramoto, and Masaya Murakami. 2004. "Guideline for Post-Earthquake Damage Evaluation and Rehabilitation of RC Buildings in Japan". Paper presented at the 13th World Conference on Earthquake Engineering. Vancouver, B.C., Canada, August 1-6.

[4] Gaetani d'Aragona, Marco, Maria Polese, Kenneth J. Elwood, Majid Baradaran Shoraka, and Andrea Prota. 2017. "Aftershock Collapse Fragility Curves for Non-Ductile RC Buildings: A Scenario-Based Assessment*." Earthquake Engineering and Structural Dynamics* 46 (13): 2083–2102. https://doi.org/10.1002/eqe.2894.

[5] Raghunandan, Meera, Abbie B. Liel, and Nicolas Luco. 2015. "Aftershock Collapse Vulnerability Assessment of Reinforced Concrete Frame Structures." *Earthquake Engineering and Structural Dynamics* 44(3): 419–39. https://doi.org/10.1002/EQE.2478.

[6] Jeon, Jong Su, Reginald Desroches, Laura N. Lowes, and Ioannis Brilakis. 2015. "Framework of Aftershock Fragility Assessment-Case Studies: Older California Reinforced Concrete Building Frames." *Earthquake Engineering and Structural Dynamics* 44(15): 2617–36. https://doi.org/10.1002/EQE.2599.

[7] Aljawhari, Karim, Roberto Gentile, Fabio Freddi, and Carmine Galasso. 2020. "Effects of Ground-Motion Sequences on Fragility and Vulnerability of Case-Study Reinforced Concrete Frames." *Bulletin of Earthquake Engineering* 1-31. https://doi.org/10.1007/s10518-020-01006-8.

[8] Gentile, Roberto, and Carmine Galasso. 2021. "Hysteretic Energy-Based State-Dependent Fragility for Ground-Motion Sequences." *Earthquake Engineering and Structural Dynamics* 50 (4): 1187–1203. https://doi.org/10.1002/eqe.3387.

[9] Gentile, Roberto, and Carmine Galasso. 2021. "Simplicity versus Accuracy Trade-off in Estimating Seismic Fragility of Existing Reinforced Concrete Buildings." *Soil Dynamics and Earthquake Engineering* 144. https://doi.org/10.1016/j.soildyn.2021.106678.

[10] Orlacchio, Mabel, Georgios Baltzopoulos, and Iunio Iervolino. 2020. "State-Dependent Seismic Fragility via Pushover Analysis." Paper presented at the 17th World Conference on Earthquake Engineering, 17WCEE Sendai, Japan.

[11] Polese, Maria, Marco Di Ludovico, Andrea Prota, and Gaetano Manfredi. 2012. "Damage-Dependent Vulnerability Curves for Existing Buildings." *Earthquake Engineering & Structural Dynamics*, 056: 1–6. https://doi.org/10.1002/eqe.

[12] Dolšek, Matjaž, and Peter Fajfar. 2004. "IN2 - A Simple Alternative for IDA." Paper presented at the 13th World Conference on Earthquake Engineering Vancouver, B.C., Canada August 1-6.

[13] Applied technology council. 996. *Seismic evaluation and retrofit of concrete buildings*. ATC 40, Redwood City, CA, USA.

[14] Nettis, Andrea, Roberto Gentile, Domenico Raffaele, Giuseppina Uva, and Carmine Galasso. 2021. "Cloud Capacity Spectrum Method: Accounting for Record-to-Record Variability in Fragility Analysis Using Nonlinear Static Procedures." *Soil Dynamics and Earthquake Engineering* 150. https://doi.org/10.1016/j.soildyn.2021.106829.

[15] Ludovico, Marco Di, Maria Polese, Marco Gaetani d'Aragona, Andrea Prota, and Gaetano Manfredi. 2013. "A Proposal for Plastic Hinges Modification Factors for Damaged RC Columns." *Engineering Structures* 51: 99–112. https://doi.org/10.1016/j.engstruct.2013.01.009.

[16] Priestley, MJ Nigel, Gian Michele Calvi, and Mervyn J. Kowalsky. 2007. *Displacement based seismic design of structures*. Pavia: Iuss.

[17] Jalayer, Fatemeh, Hossein Ebrahimian, Andrea Miano, Gaetano Manfredi, and Halil Sezen. 2017. "Analytical Fragility Assessment Using Unscaled Ground Motion Records." *Earthquake Engineering and Structural Dynamics* 46 (15): 2639–63. https://doi.org/10.1002/eqe.2922.

[18] Gentile, Roberto, and Carmine Galasso. 2020. "Gaussian Process Regression for Seismic Fragility Assessment of Building Portfolios." *Structural Safety* 87. https://doi.org/10.1016/j.strusafe.2020.101980.

[19] Goda, Katsuichiro. 2015. "Record Selection for Aftershock Incremental Dynamic Analysis." *Earthquake Engineering and Structural Dynamics* 44 (7): 1157–62. https://doi.org/10.1002/eqe.2513.

[20] Goda, Katsuichiro, and Colin A. Taylor. 2012. "Effects of Aftershocks on Peak Ductility Demand Due to Strong Ground Motion Records from Shallow Crustal Earthquakes." *Earthquake Engineering and Structural Dynamics* 41 (15): 2311–30. https://doi.org/10.1002/EQE.2188.

[21] Smerzini, Chiara, Carmine Galasso, Iunio Iervolino, and Roberto Paolucci. 2014. "Ground Motion Record Selection Based on Broadband Spectral Compatibility." *Earthquake Spectra* 30 (4): 1427–48. https://doi.org/10.1193/052312EQS197M.

[22] Carr, Anthol J. 2016. *RUAUMOKO2D - The Maori God of Volcanoes and Earthquakes. Inelastic Analysis Finite Element program*. Christchurch, New Zealand.

[23] Magenes, Guido, and Stefano Pampanin. 2004. "Seismic response of gravity-load designed frame systems with masonry infills." Paper presented at the 13th World Conference on Earthquake Engineering. Vancouver, B.C., Canada, August 1-6.

[24] New Zealand Society for Earthquake Engineering. 2017. *The Seismic Assessment of Existing Building – Technical Guidelines for Engineering Assessments*. NZSEE 2017, New Zealand.

[25] Saiidi, Mehdi, and Mete Avni Sozen. 1979. *Simple and complex models for nonlinear seismic response of reinforced concrete structures.* Urbana, IL: University of Illinois at Urbana-Champaign